Soft mobile robots with on-board chemical pressure generation

Cagdas D. Onal, Xin Chen, George M. Whitesides, and Daniela Rus

Abstract We wish to develop robot systems that are increasingly more elastic, as a step towards bridging the gap between man-made machines and their biological counterparts. To this end, we develop soft actuators fabricated from elastomer films with embedded fluidic channels. These actuators offer safety and adaptability and may potentially be utilized in robotics, wearable tactile interfaces, and active orthoses or prostheses. The expansion of fluidic channels under pressure creates a bending moment on the actuators and their displacement response follows theoretical predictions. Fluidic actuators require a pressure source, which limits their mobility and mainstream usage. This paper considers instances of mechanisms made from distributed elastomer actuators to generate motion using a chemical means of pressure generation. A mechanical feedback loop controls the chemical decomposition of hydrogen peroxide into oxygen gas in a closed container to self-regulate the actuation pressure. This on-demand pressure generator, called the pneumatic battery, bypasses the need for electrical energy by the direct conversion of chemical to mechanical energy. The portable pump can be operated in any orientation and is used to supply pressure to an elastomeric rolling mobile robot as a representative for a family of soft robots.

Key words: soft robotics, fluidic elastomer actuators, chemical pressure generation, distributed actuation, smart materials

Cagdas D. Onal and Daniela Rus
Computer Science and Artificial Intelligence Laboratory, Massachusetts Institute of Technology, Cambridge, MA, USA, e-mail: {cagdas,rus}@csail.mit.edu

Xin Chen and George M. Whitesides
Department of Chemistry and Chemical Biology, Harvard University, Cambridge, MA, USA e-mail: {xchen,gwhitesides}@gmwgroup.harvard.edu

1 Introduction

There is currently a need to develop robotic devices that rely upon new high-performance soft actuators. Compliance allows confirmation, which is desirable for adaptability in the device's negotiation with the world. A low minimum stiffness ensures safety in human interaction [1]. Many application areas will benefit from advances in practical soft actuation mechanisms including medical robotics, artificial muscles, and human interaction devices such as tactile or haptic interfaces.

Many candidate materials are under investigation to realize soft actuators. Many of these studies focus on materials that convert electrical energy to mechanical energy utilizing electroactive polymers [2] including dielectric elastomers [12, 8], electrostrictive polymers [14], and piezoelectric polymers [5]. The electrical operation principle of these actuators constrain their utility, as they require large electric fields or deformable electrodes [8].

In this paper, we describe a new soft mobile robot and demonstrate its locomotion. The robot relies on two novel robotic components: pressure-controlled soft actuators and a portable power source for these actuators.

The pressure-operated low-power soft actuators, called fluidic elastomer actuators (FEAs) [4] comprise synthetic elastomer films operated by the expansion of embedded channels under pressure. Pressure readily creates stresses inside the elastomer, which strains the material for actuation. Once pressurized, the actuator keeps its position with little or no additional energy consumption. The FEAs in this work consume 27.5 mJ of energy for 20.7 kPa pressure input. The stiffness of an FEA increases with applied pressure inside the embedded channels. This makes the material more resistant to disturbances once actuated. In case of a power failure, it can be designed to either go limb or keep its last position, both of which may be useful for safety in different scenarios.

Pressure is a convenient actuation source as it induces local deformation in a soft substrate [19], giving a large actuation range limited only by the mechanical strength of the material. In general, using direct mechanical energy in the form of pressure bypasses the need for electrical energy and its constraints. On the other hand, an important limitation on fluidic actuation is the necessity of a pressure source [7].

Our solution is to utilize a chemical approach to achieve portable and silent pressure generation. This is the equivalent of a battery for fluidic systems as it offloads pressure generation to a controlled gas generating chemical process. Specifically, we report on-demand pressure generation by the mechanical self-regulation of the decomposition of hydrogen peroxide (H_2O_2) into oxygen (O_2) gas in a closed container. The pressure output of the pneumatic battery powers FEAs for practical applications. An aqueous H_2O_2 solution is the fuel in these devices. It provides high power and is easily replaced with a fresh solution when depleted. Pure H_2O_2 has a theoretical energy density of 2.7 kJ/g, one of highest in common monopropellant fuels. While this optimal value cannot be fully utilized at room temperature operation, it indicates the potential of H_2O_2 as a practical power source. A key feature of our portable pump design is its rotation-invariant usage, which enables the battery to operate in any orientation.

Hydrogen peroxide has been used previously as a monopropellant [21] and recently in robotics applications [18, 6, 20]. A recent work utilized H_2O_2 to build a self-powered microfluidic lab-on-a-chip system [13]. Using H_2O_2 to generate pressure has the benefit of using no conventional power source for operation. Hydrogen peroxide naturally decomposes into oxygen and water with no harmful byproducts at a slow rate. This reaction speeds up in the presence of a catalyst [15]. Once this exothermic reaction starts, it continues until all of the H_2O_2 is consumed or the catalyst is removed. In previous works, relief valves were utilized to periodically vent the gas to keep the pressure build-up under control [18].

The contributions of this work are as follows:

- Modeling, design, fabrication, and evaluation of fluidic elastomer actuators.
- Modeling, design, fabrication, and evaluation of a portable power source for the actuators.
- A robot built using six FEAs and one portable power source, and locomotion experiments.

The organization of this paper is as follows. Section 2 briefly outlines the architecture of a soft robot that utilizes fluidic actuation for mobility and/or manipulation. We identify components that need to be developed to realize such a robot. In Section 3 we describe and analyze a bending-type composite fluidic elastomer actuator theoretically and experimentally. In Section 4, we present a method of self-regulation of the catalyzed decomposition of hydrogen peroxide using a mechanical feedback loop that controls the reaction based on the pressure inside the pump. We present the theory behind this concept and experimentally verify its operation. Finally, in Section 5, we illustrate the application of the pneumatic battery to power a rolling mobile robot made of six bending FEAs. The result is a complete chemically powered fluidic elastomer actuation system.

2 Soft Robot Architecture

The basic architecture of a soft robot made of fluidic actuators is shown in Fig. 1. The soft robot architecture includes all the traditional components of a robot system (*i.e.* control, perception, actuation). The unique modules are the fluidic actuator system, the pressure source for the actuators, and the interface of the actuators to the robot's control system.

The actuation power source for this application needs to be a pressure generation device that is portable in order to be incorporated in the robotic body. Support hardware comprises miniature valves that are also preferably energy-efficient. The next section describes the actuation modules for the soft robot.

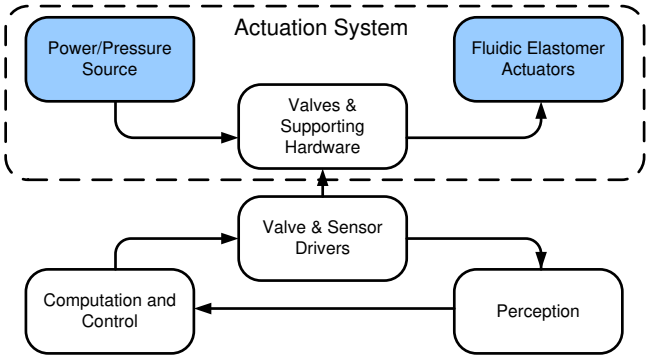

Fig. 1 The architecture of a soft robot using fluiding actuation. Components addressed in this work are shaded in blue.

3 Fluidic Elastomer Actuators Modeling and Experiments

The operational principle behind our design for FEAs relies on using pressure for actuation. In an elastomeric substrate, expansion of embedded fluidic channels due to pressure input creates overall deformation of the actuator. By the inclusion of appropriate physical constraints, this deformation is forced to follow desired motions.

The design of bending FEAs utilized in this work is shown in Fig. 2. Parallel rectangular fluidic channels reside inside the elastomeric film. The channels are connected on two ends in a meandering arrangement. Without any constraints, the material tends to undergo tensile deformation. With an inextensible thin layer placed on one side, we can convert this axial deflection to an out-of-plane bending motion. Using certain patterns of constraints, we can also induce torsion or localized deformations on the same material.

The FEAs were fabricated by molding in two layers. Molds were created using a Stratasys^{TM} Prodigy Plus^{TM} fused deposition modeling system. The first layer was a 5 mm thick elastomer with open channels on one side. The second layer was a 1.3 mm thick solid elastomer, same length and width as the first piece. The two pieces were attached together in the thickness direction using an uncured thin layer of the same material as glue such that the open channels were sealed off. For a bending actuator, the second layer also embedded a fabric mesh as an inextensible thin sheet to constrain the axial deformation of this layer. The curing time for each step was about 24 h.

Note that FEAs are modular in nature, such that placing these actuators in various arrangements yield a multitude of functionalities. Some of these functionalities are demonstrated in Fig. 3. A parallel combination of bending actuators creates a 1-D linear positioner. Placing two bending actuators together in such a way that they sandwich and share a single inextensible layer yields bidirectional bending. A serial arrangement of these bidirectional bending FEAs in alternating bending directions create a soft kinematic chain similar to an octopus arm.

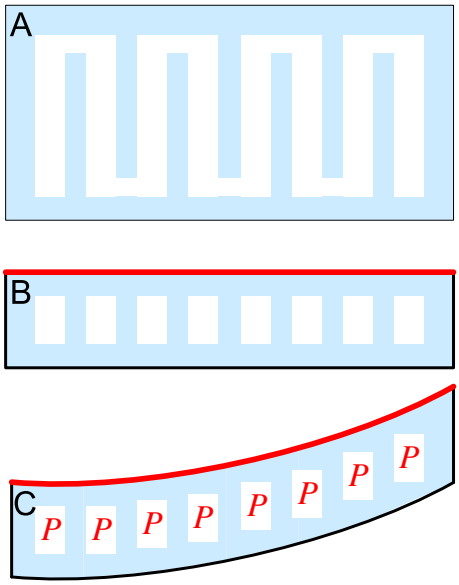

Fig. 2 The design of bending-type fluidic elastomer actuators. Fluidic channels are embedded in the elastomer and an inextensible thin layer is placed on the top (depicted in red) to induce bending. Top- and side-view sketches of the actuator are shown in *A* and *B*, respectively. The bending motion due to the pressure in the channels is depicted in *C*.

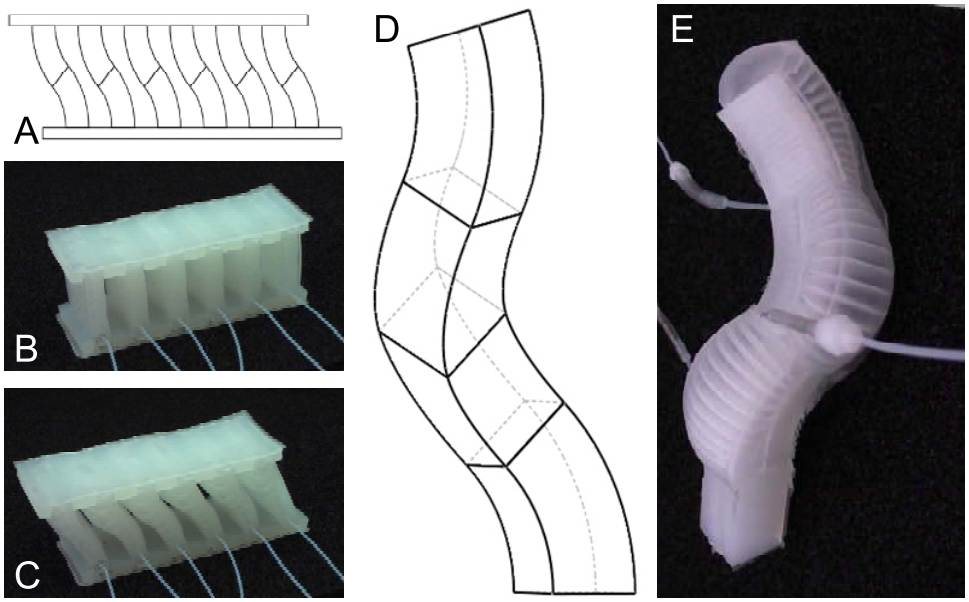

Fig. 3 (*A*-*C*) A soft linear actuator made of twelve fluidic elastomer bending actuators. (*D*-*E*) A soft kinematic chain made of four bidirectional fluidic elastomer bending actuators arranged in series.

In what follows, we derive a basic static model of displacement based on the geometry and material properties of the actuator. Applied pressure P inside the rectangular channels with height h_c and length l_c creates axial stresses σ_x in the material with height h_t and length l_t given as:

$$\sigma_x = P\frac{h_c}{h_t - h_c}. \tag{1}$$

The resulting strain ε_x is a nonlinear function of the induced stresses. The total axial deformation δ_x of the material is the combination of the individual expansions of n channels resulting in:

$$\delta_x = nl_c\varepsilon_x(\sigma_x). \tag{2}$$

In this case, the elastomer is further constrained by an inextensible thin sheet on one side, which causes the actuator to undergo bending deformation. The inextensible sheet constitutes the neutral axis of bending in the composite. Thus, the total bending angle θ can be calculated from the contributions of each channel as:

$$\theta = 2n\arctan\frac{l_c\varepsilon_x(\sigma_x)}{2h_c}. \tag{3}$$

Finally, the total out-of-plane displacement δ_y of the actuator under these conditions is written as:

$$\delta_y = \frac{l_t}{\theta}(1-\cos\theta). \tag{4}$$

The experimental setup for the investigation of the bending displacement of an FEA under pressure input is shown in Fig 4. The actuator is clamped on one end and pressure is supplied to the fluidic channels from the side at the base. The out-of-plane bending deflection is measured by image processing of a calibrated camera feed.

The bending displacement measurements in Fig. 4 were made by image processing in Matlab, using a Logitech$^{\text{TM}}$ Webcam Pro 9000 camera attached to a custom setup, clamping the FEAs on one end and tracking the tip of the actuator using color segmentation. The vertical position of the actuator tip was tracked for this measurement. FEAs were placed vertically, such that the bending axis coincided with the direction of gravity. Pressure measurements were made in Matlab, using a Honeywell$^{\text{TM}}$ ASDX030 gage pressure sensor and a National Instruments$^{\text{TM}}$ NI USB-6008 data acquisition system.

The elastomer samples used for the experiments were 38.1 mm long, 38.1 mm wide, and 6.35 mm thick stripes of Smooth-on$^{\text{TM}}$ Ecoflex$^{\text{TM}}$ Supersoft 0030 silicone rubber. They embedded 13 fluidic channels that were 1 mm long, 33 mm wide, and 3 mm thick.

The experimental deflection response of a silicone rubber FEA for pressure inputs ranging from 1 psi to 3 psi (6.9 to 20.7 kPa) is depicted in Fig. 5 with the corresponding simulation results according to the given model shown by the dashed

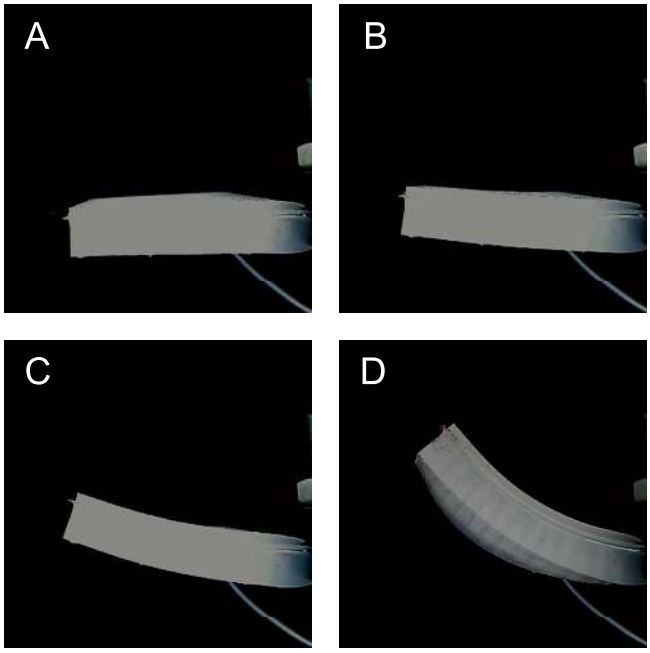

Fig. 4 Photo sequence of a fluidic elastomer bending actuator with large actuation range. As the pressure increases from 0 psi in *A* to 3 psi in *D*, the embedded channels expand laterally and bend the composite due to an inextensible thin sheet on the top layer. Upon removal of the pressure, the initial configuration in *A* is restored. Input pressure values are 1, 2, and 3 psi (6.9, 13.8, and 20.7 kPa) from *B* to *D*, respectively. The expansion of fluidic channels is visible in *D*.

curve. The stress-strain relationship of the material is determined by a power function fit to the experimental true stress and strain data.

4 Self-regulated Pressure Generation

The FEAs require a small pressure source of comparable size. In this section, we describe the design, modelling and implementation of a chemically operated portable pressure source we call a pneumatic battery.

The pneumatic battery mechanism that enables self-regulation in pressure generation from an aqueous H_2O_2 solution is depicted in Fig. 6 with a sketch and corresponding prototype. 50% wt. H_2O_2 solutions were acquired from Sigma-Aldrich^{TM} and diluted with deionized water as needed.

The pump has a cylindrical body, which makes it rotationally invariant. On one side resides an elastomeric deflector that embeds a cylindrical air chamber at atmospheric pressure sealed off from the pump by a thin circular membrane. The deflec-

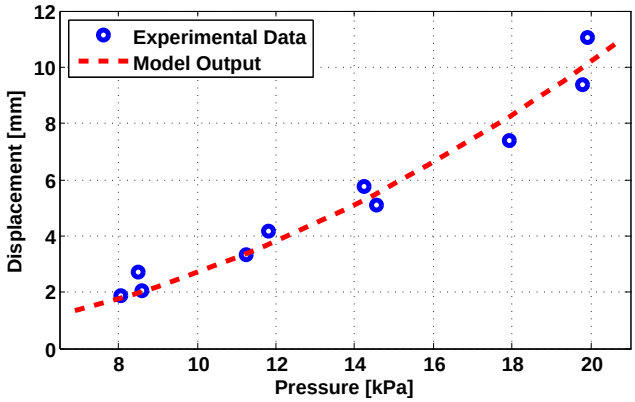

Fig. 5 Out-of-plane displacement of a fluidic elastomer actuator versus the measured pressure input. Hollow blue circles are experimental data. The dashed curve is the model output. The nonlinearity in this curve stems from the stress-strain relationship of the polymer.

tion of the membrane is dependent upon the pressure in the pump. Self-regulation is achieved by this deflection, creating a mechanical feedback loop.

As catalyst, 0.2 mm thick sheets of 92.5% pure silver (Ag) are placed on the deflector, around the membrane. The membrane is offset from another disk-shaped elastomeric layer with a boss by a defined distance. With increasing pump pressure, the membrane deflects inside and pulls the soft layer towards the catalyst pack. At a cut-off pressure value, the opposite layer completely conforms to the catalyst surface and stops the reaction. The deflector was molded in two parts from Ecoflex^{TM} 0030 silicone rubber and glued using an uncured thin layer of the same material such that the air chamber was sealed off. The air chamber inside the deflector was sealed at ambient conditions.

An outlet is placed on the other side of the pump to use the generated gas pressure for actuation. The gas is filtered by a polytetrafluoroethylene (PTFE) membrane with sub-micron pores. The filters were Whatman^{TM} 7582-004 WTP Range PTFE membranes with 47 mm diameter and 0.2 μm pore size. The hydrophobic nature of this filter keeps the solution inside the pump while allowing the gas to be removed. The rotational invariance of the mechanism makes it a good candidate for devices that do not necessarily have a defined constant direction of gravity, since it is operational in any orientation.

The prototype shown in Fig. 6 is made from a cylindrical hollow acrylic container 50.8 mm diameter and 3.2 mm thickness, laser machined acrylic lids and custom silicone rubber seals. The deflector is attached to the left lid. The PTFE filter and a pipe fitting are placed on the right lid.

The critical pressure of the pump P_c is tuned based on the following theoretical study. Static plate deflection theory predicts that the deflection w of a clamped circular membrane with radius r_m under a pressure difference $\Delta P = P_c - P_{in}$ is:

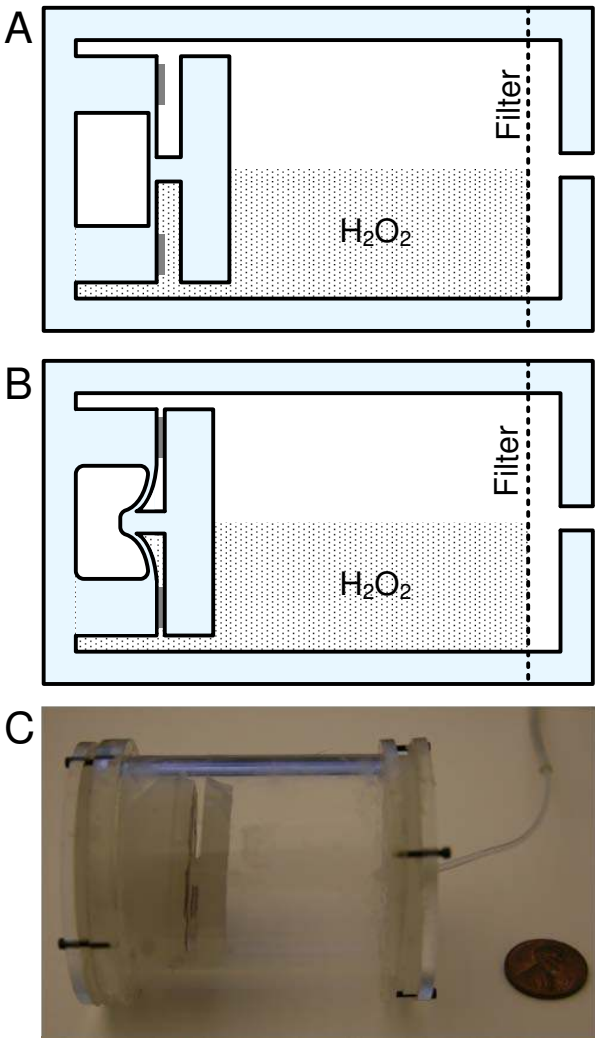

Fig. 6 Side-view sketches (*A,B*) and the prototype (*C*) of the self-regulating chemical pneumatic pump mechanism, using hydrogen peroxide as a fuel. A deflector on the left side deforms with increasing pressure and completely seals off the catalyst pack (gray) from the solution at a tuned critical pressure in *B*, effectively stopping the reaction. The gas is filtered through a hydrophobic membrane filter on the right side before the outlet.

$$w(r) = \frac{\Delta P r_m^4}{64K}\left(1 - \left(\frac{r}{r_m}\right)^2\right)^2, \tag{5}$$

where K is the flexural rigidity and ν is the Poisson's ratio of the plate. If the air chamber is connected to the atmosphere, its internal pressure P_{in} remains constant and this equation is enough to engineer the necessary amount of offset or membrane thickness for a given target cut-off pressure. For safety, to reduce the possibility of H_2O_2 leakage, this work uses a closed air chamber.

Consequently, the membrane deflection decreases the volume of the air chamber and increases its internal pressure due to the ideal gas law. With sufficiently thick walls, the volume V of the air chamber with initial height h is solely due to the membrane deflection. The pressure dependant chamber volume is written by integrating Eq. 5 over the membrane area as:

$$V = \pi r_m^2\left(h - \frac{\Delta P r_m^4}{192K}\right). \tag{6}$$

From ideal gas law, air chamber internal pressure must satisfy:

$$\frac{r_m^4}{192K}P_{in}^2 + \left(h - \frac{P_c r_m^4}{192K}\right)P_{in} - hP_o = 0, \tag{7}$$

where P_o is the initial pressure of the air chamber, typically equal to atmospheric pressure. The positive root of Eq. 7 is the final pressure in the air chamber. Given the radius of the offset boss r_o, the displacement of the opposite layer towards the catalyst pack is calculated as $w(r_o)$ from Eq. 5. We use this theory to tune the design parameters in order to achieve a certain critical pressure suitable for the FEA actuation needs.

An experimental pressure self-regulation data is displayed in Fig. 7. For this demonstration, we designed a deflector such that a silicone rubber membrane with 3 mm thickness deflects for about 2.7 mm under a critical pump pressure of 51.7 kPa (7.5 psi). We used a boss height of 2.5 mm to ensure proper conformation and sealing of the catalyst.

5 A Soft Mobile Rolling Robot Prototype powered by the Pneumatic Battery

Using the FEAs in Section 3 and the pneumatic battery in Section 4, we designed and fabricated a soft mobile robot (see Figure 8). The robot has a cylindrical body with 80 mm diameter and 63 mm length. It is made of six equally spaced bending FEAs cantilevered on the periphery of the robot, parallel to the cylinder surface. The FEAs have the same dimensions as in Section 3 and their weight is 12.5 gr. They act as flaps to bend out when actuated and apply torque, pushing the body

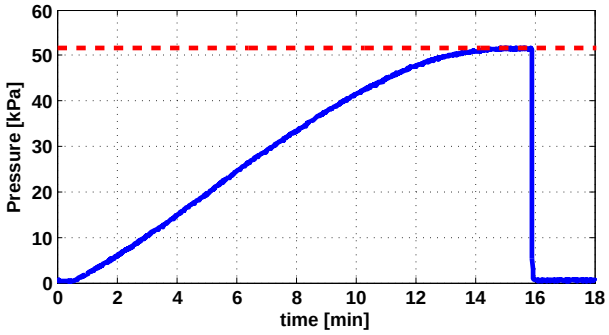

Fig. 7 Experimental results of pressure self-regulation in the pump using an approximately 10% H_2O_2 solution in water. The reaction stops at a critical pressure value of 51.7 kPa (7.5 psi) due to the deflection of the membrane sealing the catalyst off the solution. The target cut-off pressure is indicated by the dashed line. The pump is vented at 16 minutes.

forward. The actuators are fabricated separately and attached to the robot using silicone epoxy. The cylindrical body is molded from the same elastomeric material and an acrylic cylinder is placed in the center, which becomes the peroxide pump body when assembled. The total weight of the robot without the H_2O_2 solution is 210 gr.

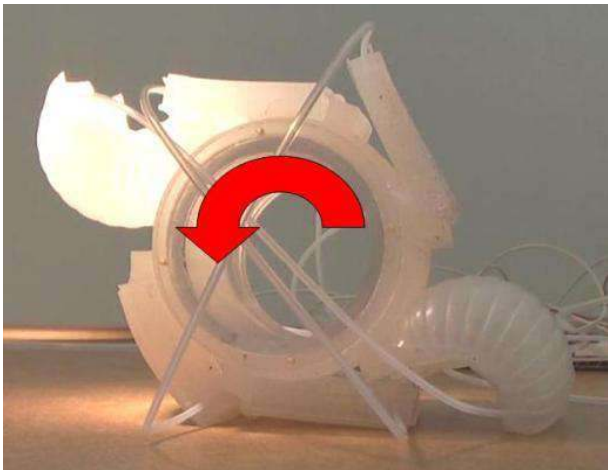

Fig. 8 Prototype of a rolling mobile robot using six bending-type fluidic elastomer actuators to propel itself forward. The hollow cylinder in the center is the housing for the pneumatic battery.

The first experiment we conducted aimed to measure the capability of the H_2O_2 pump to supply pressure to a single FEA, which is analyzed in Fig. 9. In this experiment, the pressure in the pump is measured while fluidic channels in the elastomer are pressurized and vented continuously with a 2 sec period using the generated gas.

This figure depicts that the pressure generation in the pump is canceled by the gas usage of the actuator at around 24.1 kPa (3.5 psi). This data is averaged over several hundred runs.

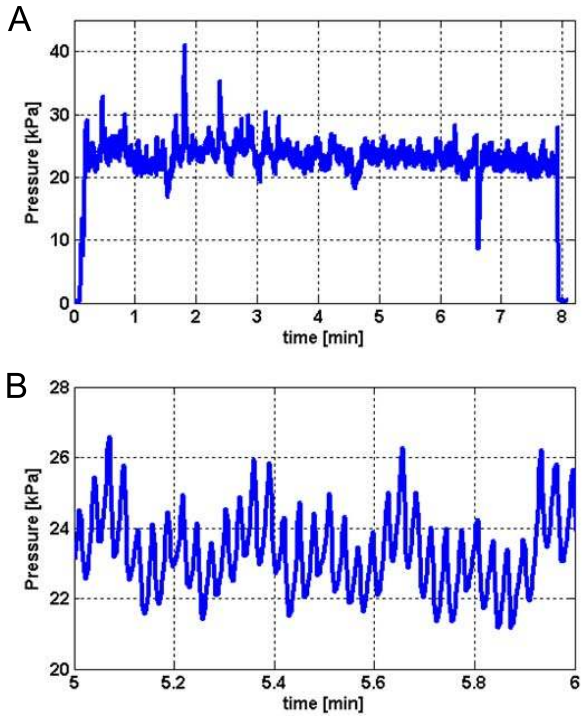

Fig. 9 Pressure inside the pump settles to a finite value while driving an FEA in *A*. Zoomed-up view of the same experiment shows spikes in the data corresponding to each actuation period in *B*.

The integration of the chemical pressure generator to functional devices made of fluidic elastomer actuators is exemplified by the hexagonal rolling mechanism with 6 FEAs in Fig. 10. The hydrogen peroxide pump rests in the center and constitutes the body and the payload of the roller in addition to providing on-board pressure. The internal volume of the pump is approximately 50 ml. A 30 ml (36 gr) fresh 50% H_2O_2 aqueous solution is used for these experiments.

The rolling motion is also selected to underline the utility of the inherent rotational invariance in this chemical pump design. This soft robotic system uses an external valve array, controlled by an operator to demonstrate the proof-of-concept of on-board pressure generation with a controlled chemical reaction.

Pressurized gas taken from the outlet fitting at the center of the pump feeds the external solenoid valve array. In this experiment, we actuated each FEA manually to induce rolling. It takes 7 sec for a single rolling step. The body travels at approx-

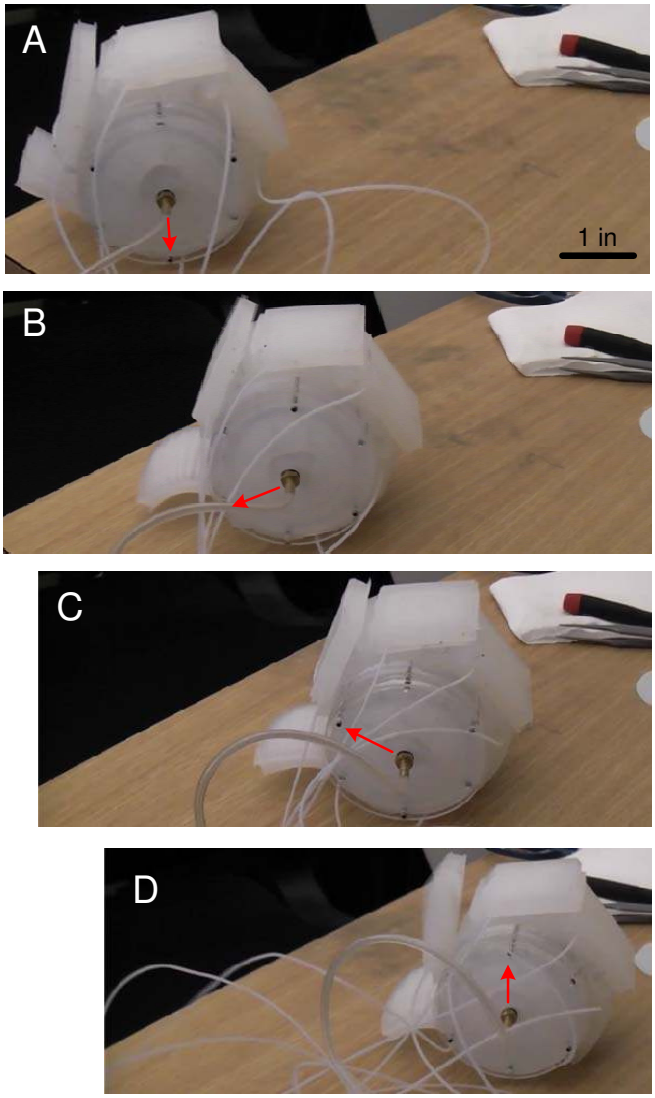

Fig. 10 Photo sequence of a pneumatic rolling mechanism made from six FEAs, rolling on a flat surface using pressure generated by an on-board hydrogen peroxide pump. Three rolling steps are shown from *A* to *D*. The actuated flaps visible in *B-D* generate the necessary force to take one rolling step. The output tubing from the pump coils with each rolling step. Red arrows are augmented to better illustrate the motion.

imately 40.2 mm for each rolling step. Even though the pneumatic battery keeps generating pressure, we did not exceed one full rotation in this experiment since the robot is tethered to the valve array.

Finally, to achieve a fully autonomous soft mobile robot, we fabricated a prototype roller with embedded valves and control as shown in Fig. 11. Six commercial solenoid latching valves are embedded in the elastomeric body under each FEA. A circular custom PCB equipped with an ATtiny13A microcontroller and driving electonics handle the control logic. The electronics and valves have low power requirements, suitable to operate from miniature LiPoly batteries. The valves are activated in a time sequence with a period of 10 sec for each rolling step. This robot can roll itself on a flat surface without user intervention.

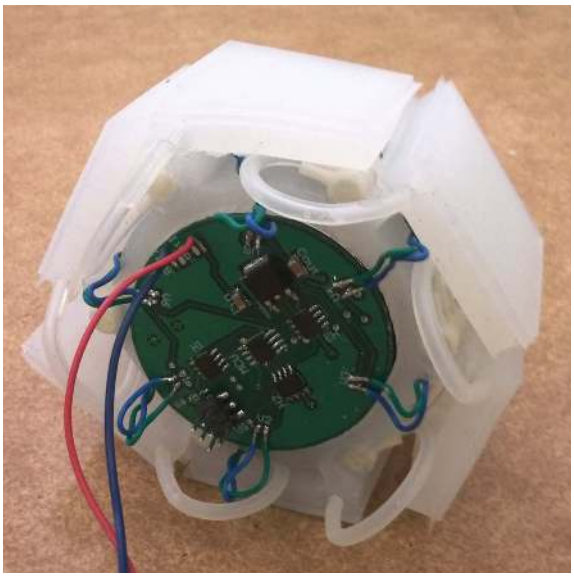

Fig. 11 Soft mobile roller prototype with on-board control electronics and embedded valves.

6 Discussion

We discussed a soft robot that uses a class of pressure-operated soft actuators, tagged the fluidic elastomer actuators (FEAs). The soft mobile robot consisted of 6 FEAs that bend out and roll the body forward. We observed that an algorithm that actuates the FEAs in sequence induces rolling locomotion of such a soft robotic design.

We theoretically analyzed and experimentally studied the displacement response of bending-type FEAs. The resulting theory provided insight to FEA operation based on the geometry and material properties of the elastomer. Pressure gener-

ation was offloaded to a chemical process, namely the catalyzed decomposition of hydrogen peroxide. With a unique mechanical self-regulation mechanism, this chemical reaction is controlled to keep the pressure constant at a predefined value. This chemomechanical generator, called the pneumatic battery, powered FEAs with no electrical energy consumption as a proof-of-concept demonstration.

Silent and portable operation of this mechanism provides an important step towards the common application of soft fluidic actuators in functional devices. The cheap and fast fabrication of FEAs in addition to their inherent safety makes them useful in human interactions. Potential applications include artificial muscles [17], assistive or rehabilitative devices, haptic or tactile displays and interfaces. Such applications will benefit from a distributed arrangement of these actuators in arbitrary 3D shapes.

Silver oxidizes when exposed to air, which leads to catalyst degradation. Switching to an alternative catalyst such as platinum may be one solution. Also, it has been suggested that a high pH may help this reaction and tin becomes an effective catalyst in a basic solution [18]. A thorough investigation of the pressure build-up rate in the pump for different catalysts and pH values is necessary for optimized operation.

We haven't considered the temperature in the pump. Especially for high H_2O_2 concentrations, the temperature increase becomes large and affects the cut-off pressure value. An open air chamber would circumvent this problem, with a loss of safety from peroxide leakage.

While we demonstrated pressure generation in a practical size, some open questions remain to be answered. For example, can we further miniaturize this chemical pump such that it is embedded inside the elastomer substrate? Microfabrication technologies certainly offer the means to build scaled-down versions of the same design. The catalyst area, however, would be much smaller for a millimeter scale prototype. A distributed structure with many mini-pumps working in parallel may be helpful. On the other hand, a change in the current design to utilize a scaled-down Kipp generator to constitute the self-regulation mechanism in smaller scales seems promising.

Currently, commercial solenoid valves drive the actuators. We are interested in miniature valves that can be embedded in the actuator body itself to achieve a fully embedded actuation system that is directly addressable. Recent studies on microfabricated valves [11, 10] and microfluidic multiplexers [16] provide some options. We recently developed custom compact and energy-efficient valves controlled by electropermanent magnets to this end [9].

Similarly, we are interested in soft sensing elements that can be placed inside the FEAs. These sensors will provide feedback on the shape of the actuator and improve controllability [3].

Acknowledgements This work was done in the Distributed Robotics Laboratory at MIT with partial support from the DARPA DSO "Chembots" project (W911NF-08-C-0060). We are grateful to DARPA and to our collaborators.

References

1. Albu-Schaffer, A., Eiberger, O., Grebenstein, M., Haddadin, S., Ott, C., Wimbock, T., Wolf, S., Hirzinger, G.: Soft robotics. IEEE Robotics & Automation Magazine **15**, 20–30 (2008)
2. Bar-Cohen, Y.: Electroactive Polymer EAP Actuators as Artificial Muscles: Reality, potential and challenges. SPIE Press, 2nd edition (2004)
3. Chiechi, R.C., Weiss, E.A., Dickey, M.D., Whitesides, G.M.: Eutectic gallium-indium (egain): A moldable liquid metal for electrical characterization of self-assembled monolayers. Angewandte Chemie **47**, 142–144 (2008)
4. Correll, N., Onal, C.D., Liang, H., Schoenfeld, E., Rus, D.: Soft autonomous materials - using active elasticity and embedded distributed computation. In: 12th Internatoinal Symposium on Experimental Robotics. New Delhi, India (2010)
5. Fu, Y., Harvey, E.C., Ghantasala, M.K., Spinks, G.M.: Design, fabrication and testing of piezoelectric polymer pvdf microactuators. Smart Materials and Structures **15**(1), S141 (2006)
6. Goldfarb, M., Barth, E.J., Gogola, M.A., Wehrmeyer, J.A.: Design and energetic characterization of a liquid-propellant-powered actuator for self-powered robots. IEEE/ASME Transactions on Mechatronics **8**(2), 254–262 (2003)
7. Kazerooni, H.: Design and analysis of pneumatic force generators for mobile robotic systems. IEEE/ASME Transactions on Mechatronics **10**(4), 411–418 (2005)
8. Keplinger, C., Kaltenbrunner, M., Arnold, N., Bauer, S.: Rntgens electrode-free elastomer actuators without electromechanical pull-in instability. PNAS **107**(10), 4505–4510 (2010)
9. Marchese, A., Onal, C.D., Rus, D.: Soft robot actuators using energy-efficient valves controlled by electropermanent magnets. In: IEEE/RSJ International Conference on Intelligent Robots and Systems (IROS) (2011 (to appear))
10. Mosadegh, B., Kuo, C.H., Tung, Y.C., Torisawa, Y.s., Bersano-Begey, T., Tavana, H., Takayama, S.: Integrated elastomeric components for autonomous regulation of sequential and oscillatory flow switching in microfluidic devices. Nature Physics **6**(6), 433–437 (2010)
11. Oh, K.W., Ahn, C.H.: A review of microvalves. Journal of Micromechanics and Microengineering **16**(5), R13 (2006)
12. Pelrine, R., Kornbluh, R., Pei, Q., Joseph, J.: High-Speed Electrically Actuated Elastomers with Strain Greater Than 100%. Science **287**(5454), 836–839 (2000)
13. Qin, L., Vermesh, O., Shi, Q., Heath, J.R.: Self-powered microfluidic chips for multiplexed protein assays from whole blood. Lab on a Chip **9**, 2016–2020 (2009)
14. Richards, A.W., Odegard, G.M.: Constitutive modeling of electrostrictive polymers using a hyperelasticity-based approach. Journal of Applied Mechanics **77**(1), 014502 (2010)
15. Salem, I.A., El-Maazawi, M., Zaki, A.B.: Kinetics and mechanisms of decomposition reaction of hydrogen peroxide in presence of metal complexes. Int J Chem Kin **32**(11), 643–666 (2000)
16. Thorsen, T., Maerkl, S.J., Quake, S.R.: Microfluidic Large-Scale Integration. Science **298**(5593), 580–584 (2002)
17. Trivedi, D., Rahn, C., Kier, W., Walker, I.: Soft robotics: Biological inspiration, state of the art, and future research. Advanced Bionics and Biomechanics **5**(2), 99–117 (2008)
18. Vitale, F., Accoto, D., Turchetti, L., Indini, S., Annesini, M.C., Guglielmelli, E.: Low-temperature h2o2-powered actuators for biorobotics: thermodynamic and kinetic analysis. In: Proc. IEEE Int. Conf. on Robotics and Automation, pp. 2197–2202 (2010)
19. Wait, K., Jackson, P., Smoot, L.: Self locomotion of a spherical rolling robot using a novel deformable pneumatic method. In: Robotics and Automation (ICRA), 2010 IEEE International Conference on, pp. 3757–3762 (2010)
20. Wang, Y., Hernandez, R.M., D. J. Bartlett, J., Bingham, J.M., Kline, T.R., Sen, A., Mallouk, T.E.: Bipolar electrochemical mechanism for the propulsion of catalytic nanomotors in hydrogen peroxide solutions. Langmuir **22**, 10,451–10,456 (2006)
21. Whitehead, J.C.: Hydrogen peroxide propulsion for smaller satellites. In: Proc. AIAA/USU Conference on Small Satellites (1998)